Journal of Engineering Mathematics **50:** 75–93, 2004.

Buckling of fiber-reinforced viscoelastic composite plates using various plate theories

A.M. ZENKOUR
Department of Mathematics, Faculty of Education, Tanta University, Kafr El-Sheikh 33516, Egypt
E-mail: Zenkour@powernet.com.eg

Received 10 February 2003; Accepted in revised form 8 April 2004

Abstract. This paper studies the quasi-static stability analysis of fiber-reinforced viscoelastic composite plates subjected to in-plane edge load systems. The study is based on a unified shear-deformable plate theory. This theory enables the trial and testing of different through-thickness transverse shear-strain distributions and, among them, strain distributions that do not involve the undesirable implications of the transverse shear correction factors. Using the method of effective moduli solves the equations governing the stability of simply supported fiber-reinforced viscoelastic composite plates. The solution concerns the determination of the critical in-plane edge loads associated with the asymptotic instability of plates. In a study of this problem the general quasi-static stability solutions are compared with those based on the classical, first-order and sinusoidal transverse shear-deformation theories. Numerical applications using higher-order shear-deformation theory are presented and comparisons with the results of other theories are formulated.

Key words: critical buckling load, effective moduli, quasi-static, unified theory

1. Introduction

Advanced fiber-reinforced composites have gained increasing attention in recent years. This attention is due to their widespread use in modern aerospace transportation systems and in other areas of high performance. The composite material structures exhibit time-dependent properties which could be modeled by a linear (or nonlinear) constitutive law. In addition, these composite material structures exhibit a weak rigidity in transverse shear that requires the incorporation of transverse shear-deformation effects.

Elastic properties of multi-phase composite materials have been studied extensively. Among these studies are those dealing with bounds on the elastic behaviour and predicted properties of composites of relatively simple structures. The upper and lower bounds of stiffness of two-phase and many-phase composite materials have been obtained in terms of volume fraction of constituents (see, *e.g.*, [1] and [2]). Bounds and expressions for the effective elastic moduli of materials reinforced by parallel hollow circular fibers in hexagonal or random arrays have also been derived by a variational method [1]. Furthermore, bounds on three independent effective elastic moduli of an *n*-phase fiber-reinforced composite of arbitrary transverse phase geometry, plane-strain bulk modulus, transverse shear modulus and shear modulus in plane parallel to fibers, have been derived in terms of phase volume fractions [3]. For viscoelastic heterogeneous media of several discrete linear viscoelastic phases with known stress-strain relations, it has been shown that the effective relaxation and creep functions can be obtained by the corresponding principle of the theory of linear viscoelasticity. In some cases explicit results in terms of general linear viscoelastic matrix properties have been given,

thus permitting direct use of experimental information [4]. In a review by Ahmed and Jones [5] of particulate reinforcement theories for polymer composites, it was concluded that the size, shape, distribution, and interfacial adhesion of the inclusions affected the macroscopic behaviour.

The stability of rectangular, viscoelastic, orthotropic plates subjected to biaxial compression was analyzed by Wilson and Vinson [6]. In their analysis, the equations governing the stability were obtained by using the quasi-elastic approximation, which overlooks the hereditary material behaviour. Kim and Hong [7] examined the viscoelastic-buckling load of sandwich plates with cross-ply faces. Huang [8] studied the viscoelastic buckling and post-buckling of circular cylindrical laminated shells. These works, as in [6], were conducted within the framework of the quasi-elastic analysis, *i.e.*, the buckling load and post-buckling deflection are obtained by direct substitution of time-varying properties in the elastic formulations of the problem. Pan [9] analyzed the dynamic response problem of isotropic viscoelastic plates by extending, for this case, Mindlin's shear-deformation plate theory. Librescu and Chandiramani [10] presented a paper that deals with the dynamic stability analysis of transversely isotropic viscoelastic plates subjected to in-plane biaxial edge-load systems. In their derivation of the associated governing equations they used a Boltzmann hereditary constitutive law and, in addition, transverse shear deformation, transverse normal stress and rotatory inertia effects were incorporated.

This paper deals with a quasi-static stability analysis of fiber-reinforced viscoelastic rectangular plates subjected to in-plane edge-load systems. In deriving the governing equations, the effective-moduli method was used and, in addition, transverse shear-deformation effects were incorporated. Numerical results of critical buckling loads are presented, comparisons with the existing literature are made, and conclusions are formulated.

2. Theory and formulation

The simplest case of a two-phase composite represents rigorous upper and lower bounds on Young's modulus for a given volume fraction of one phase. The geometry of such model structure is shown in Figure 1. The composite can contain laminations as shown in Figure 1 or it can be made of continuous fibers; in either case the strain is the same in each phase. For an elastic material with one of these structures, Young's modulus of the composite is given by the relation $E_c = \gamma_1 E_1 + \gamma_2 E_2$, in which E_1 and E_2 refer to Young's moduli of phase 1

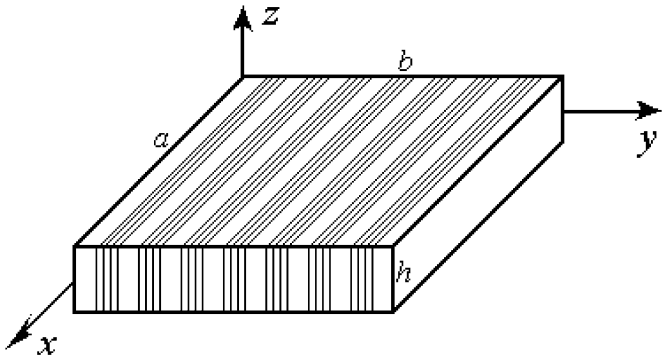

Figure 1. A fiber-reinforced viscoelastic rectangular plate.

and phase 2, respectively. Also γ_1 and γ_2 refer to the volume fraction of the two phases with $\gamma_1 + \gamma_2 = 1$.

The fiber-reinforced two-phase composite plate as shown in Figure 1 is assumed to be of uniform thickness h and made of a material composed of two components. One of these (phase 1) is an elastic material with modulus of elasticity E_r and Poisson's ratio ν_r. The other component (phase 2) may possess either elastic properties with modulus E_f and Poisson's ratio ν_f or the properties of a linear isotropic viscoelastic material characterized by the modulus of bulk K which is assumed to be constant and the dimensionless parameter $\bar{\omega}$. So, phase 1 will serve as the reinforcement, while phase 2 will play the role of the filler.

The rectangular Cartesian planform co-ordinates x and y are introduced in the deformation analysis of the present plate. The considered plate is bounded by the coordinate planes $x = 0$, a and $y = 0$, b. The reference surface is the middle surface of the plate defined by $z = 0$, and z denotes the thickness co-ordinate measured from the undeformed middle surface.

The displacements of a material point located at (x, y, z) in the plate may be written as (see [11]):

$$u_1 = u - z\frac{\partial w}{\partial x} + \Psi(z)\varphi_1, \qquad u_2 = v - z\frac{\partial w}{\partial y} + \Psi(z)\varphi_2, \qquad u_3 = w, \tag{1}$$

where (u_1, u_2, u_3) are the displacements corresponding to the co-ordinate system and are functions of the spatial co-ordinates; (u, v, w) are the displacements along the axes x, y and z, respectively, and φ_1 and φ_2 are the rotations about the y- and x-axes. All of the generalized displacements $(u, v, w, \varphi_1, \varphi_2)$ are functions of (x, y). The shape function $\Psi(z)$ is to be specified *a posteriori* [12]. It may be chosen such that

$$\Psi'(z) = 0 \qquad at \qquad z = \pm h/2, \tag{2a}$$

and/or

$$\int_{-h/2}^{+h/2} \Psi(z)\mathrm{d}z = 0. \tag{2b}$$

The first condition in (2) means that the transverse shear strain vanishes on the bounding planes $z = \pm h/2$. The shear deformation theory that satisfies this condition does not require any shear-correction factors. In general, the second condition in (2) may be satisfied for most two-dimensional theories.

The six strain components compatible with the displacement field in (1) are

$$\begin{aligned} &\varepsilon_i = \varepsilon_i^0 + z\kappa_i + \Psi(z)\eta_i, \quad (i = 1, 2, 6), \\ &\varepsilon_3 = 0, \quad \varepsilon_j = \Psi'(z)\,\varepsilon_j^0, \quad (j = 4, 5), \end{aligned} \tag{3}$$

where

$$\begin{aligned} &\varepsilon_1^0 = \frac{\partial u}{\partial x}, \quad \varepsilon_2^0 = \frac{\partial v}{\partial y}, \quad \varepsilon_4^0 = \varphi_2, \quad \varepsilon_5^0 = \varphi_1, \quad \varepsilon_6^0 = \frac{\partial v}{\partial x} + \frac{\partial u}{\partial y}, \\ &\kappa_1 = -\frac{\partial^2 w}{\partial x^2}, \qquad \kappa_2 = -\frac{\partial^2 w}{\partial y^2}, \qquad \kappa_6 = -2\frac{\partial^2 w}{\partial x \partial y}, \\ &\eta_1 = \frac{\partial \varphi_1}{\partial x}, \qquad \eta_2 = \frac{\partial \varphi_2}{\partial y}, \qquad \eta_6 = \frac{\partial \varphi_2}{\partial x} + \frac{\partial \varphi_1}{\partial y}. \end{aligned} \tag{4}$$

It becomes clear therefore that, through its derivative, the *a posteriori* specified function $\Psi(z)$ will determine the through-the-thickness trial distribution of the transverse shear strain.

The constitutive law that relates stresses and strains in a linear viscoelastic fiber-reinforced material may be expressed in hereditary integral form in the time domain and in the polynomial form in the *Laplace* domain. For a plate, thin or moderately thick, the normal stress in the thickness direction is small and negligible. The general constitutive equations may be simplified by neglecting this normal stress. The simplified constitutive law is

$$\begin{Bmatrix} \sigma_1 \\ \sigma_2 \\ \sigma_4 \\ \sigma_5 \\ \sigma_6 \end{Bmatrix} = \begin{bmatrix} \bar{c}_{11} & \bar{c}_{12} & 0 & 0 & 0 \\ & \bar{c}_{22} & 0 & 0 & 0 \\ & & \bar{c}_{44} & 0 & 0 \\ & & & \bar{c}_{55} & 0 \\ \text{symm.} & & & & \bar{c}_{66} \end{bmatrix} \begin{Bmatrix} \varepsilon_1 \\ \varepsilon_2 \\ \varepsilon_4 \\ \varepsilon_5 \\ \varepsilon_6 \end{Bmatrix}, \tag{5}$$

where $\bar{c}_{ij}$ are the compliance constants, which depend on the material properties of the two components of the plate. Then

$$\begin{aligned} \bar{c}_{11} &= \frac{\bar{E}_x}{1-\bar{\nu}_{xy}\bar{\nu}_{yx}},\ \bar{c}_{12} = \frac{\bar{\nu}_{xy}\bar{E}_y}{1-\bar{\nu}_{xy}\bar{\nu}_{yx}} = \frac{\bar{\nu}_{yx}\bar{E}_x}{1-\bar{\nu}_{xy}\bar{\nu}_{yx}},\ \bar{c}_{22} = \frac{\bar{E}_y}{1-\bar{\nu}_{xy}\bar{\nu}_{yx}}, \\ \bar{c}_{44} &= \bar{G}_{yz},\ \bar{c}_{55} = \bar{G}_{xz},\ \bar{c}_{66} = \bar{G}_{xy}, \end{aligned} \tag{6}$$

where $\bar{E}_x$ and $\bar{E}_y$ are Young's moduli; $\bar{\nu}_{xy}$ and $\bar{\nu}_{yx}$ gre Poisson's ratios; and $\bar{G}_{xy}$, $\bar{G}_{yz}$ and $\bar{G}_{xz}$ are shear moduli. In the case in which the filler (phase 2) is a viscoelastic material, the compliance constants $\bar{c}_{ij}$ are said to be the effective relaxation kernels. Young's moduli, Poisson's ratios and shear moduli are defined in Appendix A in terms of some known kernels $\bar{g}_\chi$ constructed on the basis of the kernel $\bar{\omega}$ (see [13]). So the effective relaxations kernels $\bar{c}_{ij}$ can always be represented in the form $\bar{c}_{ij} = c_{ij}(\chi)\bar{g}_\chi$, where $c_{ij}(\chi)$ are constants.

3. Governing equations

Let the upper surface of the plate ($z = h/2$) be subjected to a transverse distribution load $q(x, y)$. Let there be distributed compressive in-plane forces S_1 and S_2 (per unit length) acting on the mid-surface of the plate.

The principle of virtual displacements for the present problem may be expressed as follows:

$$0 = \int_\Omega \left[\int_{-h/2}^{+h/2} [\sigma_1 \delta\varepsilon_1 + \sigma_2 \delta\varepsilon_2 + \ldots] dz + \left(S_1 \frac{\partial w}{\partial x}\frac{\partial}{\partial x} + S_2 \frac{\partial w}{\partial y}\frac{\partial}{\partial y} - q \right) \delta w \right] \mathrm{d}\Omega, \tag{7}$$

or

$$\begin{aligned} 0 = \int_\Omega \big[& N_1\delta\varepsilon_1^0 + N_2\delta\varepsilon_2^0 + N_6\delta\varepsilon_6^0 + M_1\delta\kappa_1 + M_2\delta\kappa_2 + M_6\delta\kappa_6 + M_1^a\delta\eta_1 + M_2^a\delta\eta_2 \\ & + M_6^a\delta\eta_6 + Q_4^a\delta\varepsilon_4^0 + Q_5^a\delta\varepsilon_5^0 + \left(S_1\frac{\partial w}{\partial x}\frac{\partial}{\partial x} + S_2\frac{\partial w}{\partial y}\frac{\partial}{\partial y} - q \right)\delta w \Big] \mathrm{d}\Omega, \end{aligned} \tag{8}$$

where N_i and M_i are the basic components of stress resultants and stress couples, M_i^a are additional stress couples associated with the transverse shear effects and Q_l^a are transverse-shear-stress resultants. Here N_i and M_i etc., can be expressed as

$$\begin{aligned} &\{N_i, M_i, M_i^a\} = \textstyle\int_{-h/2}^{+h/2} \{1, z, \Psi(z)\}\sigma_i \mathrm{d}z, \\ &Q_l^a = \textstyle\int_{-h/2}^{+h/2} \Psi'(z)\sigma_l \mathrm{d}z, \quad (i = 1, 2, 6;\ l = 4, 5). \end{aligned} \tag{9}$$

The governing equilibrium equations can be derived from (8) by integrating the displacement gradient in ε_i by parts and setting the coefficients of $\delta u, \delta v, \delta w, \delta\varphi_1$, and $\delta\varphi_2$ to zero separately. Thus one obtains

$$\delta u: \quad \frac{\partial N_1}{\partial x} + \frac{\partial N_6}{\partial y} = 0, \tag{10}$$

$$\delta v: \quad \frac{\partial N_6}{\partial x} + \frac{\partial N_2}{\partial y} = 0, \tag{11}$$

$$\delta w: \quad \frac{\partial^2 M_1}{\partial x^2} + 2\frac{\partial^2 M_6}{\partial x\,\partial y} + \frac{\partial^2 M_2}{\partial y^2} + q + \frac{\partial}{\partial x}\left(S_1\frac{\partial w}{\partial x}\right) + \frac{\partial}{\partial y}\left(S_2\frac{\partial w}{\partial y}\right) = 0, \tag{12}$$

$$\delta\varphi_1: \quad \frac{\partial M_1^a}{\partial x} + \frac{\partial M_6^a}{\partial y} - Q_5^a = 0, \tag{13}$$

$$\delta\varphi_2: \quad \frac{\partial M_6^a}{\partial x} + \frac{\partial M_2^a}{\partial y} - Q_4^a = 0. \tag{14}$$

By using (5) in (9), the force and moment resultants of the theory can be related to the total strains to yield the following constitutive equations:

$$\begin{aligned} N_i &= A_{ij}\,\varepsilon_j^0 + B_{ij}\,\kappa_j + B_{ij}^a\,\eta_j, \\ M_i &= B_{ij}\,\varepsilon_j^0 + D_{ij}\,\kappa_j + D_{ij}^a\,\eta_j, \qquad (i, j = 1, 2, 6), \\ M_i^a &= B_{ij}^a\,\varepsilon_j^0 + D_{ij}^a\,\kappa_j + F_{ij}^a\,\eta_j, \end{aligned} \tag{15a}$$

and

$$Q_l^a = A_{ll}^a\,\varepsilon_l^0, \quad (l = 4, 5). \tag{15b}$$

The following definitions are used for the stiffnesses in the above equation:

$$\begin{aligned} \{A_{ij}, B_{ij}, D_{ij}\} &= \textstyle\int_{-h/2}^{+h/2} \bar{c}_{ij}\{1, z, z^2\}\mathrm{d}z, \\ \{B_{ij}^a, D_{ij}^a, F_{ij}^a\} &= \textstyle\int_{-h/2}^{+h/2} \bar{c}_{ij}\,\Psi(z)\{1, z, \Psi(z)\}\mathrm{d}z, \\ A_{ll}^a &= \textstyle\int_{-h/2}^{+h/2} \bar{c}_{ll}[\Psi'(z)]^2\mathrm{d}z, \quad (i, j = 1, 2, 6;\ l = 4, 5). \end{aligned} \tag{16}$$

Note that, in addition to the above equilibrium and constitutive equations, the essential and natural boundary conditions may be obtained easily from (8) and they are given in Table 1:

4. Analytical solutions

In this approach, we express the generalized displacements so as to satisfy the boundary conditions representing simple support:

$$\begin{aligned} v = w = \varphi_2 = N_1 = M_1 = M_1^a = 0 \quad at \quad x = 0, a, \\ u = w = \varphi_1 = N_2 = M_2 = M_2^a = 0 \quad at \quad y = 0, b. \end{aligned} \tag{17a}$$

Table 1. Boundary conditions.

Essential	Natural
u	$N_1 n_x + N_6 n_y$
v	$N_6 n_x + N_2 n_y$
w	$\left(\frac{\partial M_1}{\partial x} + \frac{\partial M_6}{\partial y} + S_1 \frac{\partial w}{\partial x}\right) n_x + \left(\frac{\partial M_6}{\partial x} + \frac{\partial M_2}{\partial y} + S_2 \frac{\partial w}{\partial y}\right) n_y$
$\frac{\partial w}{\partial x}$	$M_1 n_x + M_6 n_y$
$\frac{\partial w}{\partial y}$	$M_6 n_x + M_2 n_y$
φ_1	$M_1^a n_x + M_6^a n_y$
φ_2	$M_6^a n_x + M_2^a n_y$

The following representation for the displacement quantities is appropriate in the analysis of the present problem:

$$\left\{\begin{array}{c} u \\ v \\ w \\ \varphi_1 \\ \varphi_2 \end{array}\right\} = \sum_{m=1}^{\infty} \sum_{n=1}^{\infty} \left\{\begin{array}{l} U_{mn} \cos(\lambda x) \sin(\mu y) \\ V_{mn} \sin(\lambda x) \cos(\mu y) \\ W_{mn} \sin(\lambda x) \sin(\mu y) \\ X_{mn} \cos(\lambda x) \sin(\mu y) \\ Y_{mn} \sin(\lambda x) \cos(\mu y) \end{array}\right\}, \tag{17b}$$

where $\lambda = m\pi/a$ and $\mu = n\pi/b$ and U_{mn}, V_{mn}, W_{mn}, X_{mn}, and Y_{mn} are arbitrary parameters. The above representation is appropriate in dealing with the (quasi-static) compressive buckling problem. The simplest case, to derive some results which concern the buckling of viscoelastic rectangular plates, is obtained when the forces S_1 and S_2 are given throughout the plate and the transversal load term is dropped ($q = 0$). Assuming that there is a given ratio between these forces, so that $S_1 = -S_0/P(t)$ and $S_2 = \alpha S_1$, we get

$$(P(t)[L] - S_0[S])\{\Delta\} = \{0\}, \tag{18}$$

where $P(t)$ is a transient function accounting for the viscoelastic response of the buckling problem and $\{\Delta\}$ denotes the column

$$\{\Delta\}^T = \{U_{mn}, V_{mn}, W_{mn}, X_{mn}, Y_{mn}\}. \tag{19}$$

The elements $L_{ij} = L_{ji}$ of matrix $[L]$ are given by:

$$\begin{aligned}
L_{11} &= A_{11}\lambda^2 + A_{66}\mu^2, \\
L_{12} &= \lambda\mu(A_{12} + A_{66}), \\
L_{13} &= 0, \\
L_{14} &= B_{11}^a\lambda^2 + B_{66}^a\mu^2, \\
L_{15} &= \lambda\mu(B_{12}^a + B_{66}^a), \\
L_{22} &= A_{66}\lambda^2 + A_{22}\mu^2, \\
L_{23} &= 0, \\
L_{24} &= L_{15}, \\
L_{25} &= B_{66}^a\lambda^2 + B_{22}^a\mu^2,
\end{aligned}$$

$$
\begin{aligned}
L_{33} &= D_{11}\lambda^4 + 2\lambda^2\mu^2(D_{12} + 2D_{66}) + D_{22}\mu^4,\\
L_{34} &= -\lambda[D^a_{11}\lambda^2 + (D^a_{12} + 2D^a_{66})\mu^2],\\
L_{35} &= -\mu[(D^a_{12} + 2D^a_{66})\lambda^2 + D^a_{22}\mu^2],\\
L_{44} &= F^a_{11}\lambda^2 + F^a_{66}\mu^2 + A^a_{55},\\
L_{45} &= \lambda\mu(F^a_{12} + F^a_{66}),\\
L_{55} &= F^a_{66}\lambda^2 + F^a_{22}\mu^2 + A^a_{44}.
\end{aligned}
$$

All elements of matrix $[S]$ are zeros, except $S_{33} = \lambda^2 + \alpha\mu^2$. For non-trivial solutions of (20), the following determinant should be zero

$$|P(t)[L] - S_0[S]| = 0. \tag{20}$$

This equation gives the buckling loads. Note that the assumed buckling of the plate is possible only for definite values of S_0. The smallest of these values determines the desired critical value.

4.1. Biaxial compression of a viscoelastic plate

For a viscoelastic composite rectangular plate subjected to the same magnitude of uniform compressive forces S_1 and S_2 on both edges (*i.e.*, biaxial compression), we may calculate the buckling load using (20) with $\alpha = 1$.

4.2. Uniaxial compression of a viscoelastic plate

When the viscoelastic composite rectangular plate is subjected to uniform compressive load S_1 on the edges $x = 0$ and $x = a$, we may calculate the buckling load using (20) with $\alpha = 0$.

4.3. Buckling of a viscoelastic plate under combined bending and compression

The problem becomes more involved if either of the forces S_1 or S_2 varies along one coordinate direction. Let us consider a simply supported viscoelastic rectangular plate with distributed in-plane forces applied in the middle plane of the plate on sides x = 0, a only, *i.e.*, $S_2 = 0$. The distribution of the applied force is given, for example, by

$$S_1 = -\frac{S_0}{P(t)}\left(1 - c\frac{y}{b}\right), \tag{21}$$

where c is a numerical factor. In this case (18) has variable coefficients, but the general conclusion remains the same. The elements of $[L]$ and $[S]$ are still the same except $S_{33} = \lambda^2(1-c/2)$. By changing the factor c one obtains various particular cases. For example, $c = 0$ corresponds to the case of uniformly distributed compressive force ($S_1 = -S_0/P(t),\ \alpha = 0$) and for $c = 2$ we obtain the case of pure bending. All other values give a combination of bending and compressive ($c < 2$) or tension ($c > 2$).

4.4. The shape function $\Psi(z)$

It is known that the classical plate theory based on the Love-Kirchhoff assumptions is only adequate for predicting the gross behaviour of a thin plate [14], [15, pp. 76–138], [16]). When

the structures are rather thick, the transverse shear-deformation effect has to be incorporated. In such cases more refined theories are needed (see, *e.g.*, [16–19], [20, pp. 353–371], [21–23], [24, pp. 351–360]).

Most of the solutions shown were based on choices of the shape function $\Psi(z)$ that are consistent with the so-called higher-order shear-deformation plate theory (HPT). For comparison purposes, however, two more choices of the shape functions are also used. These are consistent with the so-called first-order (uniform) shear-deformation plate theory (FPT) and a shear-deformable theory that uses a shape function of sinusoidal type (SPT). In some cases, involving zero shape function, the classical plate theory (CPT) has also been used for comparison purposes. In more detail, the shape function employed for each theory is as follows:

$$\begin{aligned}
&\text{CPT}: \ \Psi(z) = 0,\\
&\text{FPT}: \ \Psi(z) = z,\\
&\text{SPT}: \ \Psi(z) = \tfrac{h}{\pi}\sin\left(\tfrac{\pi z}{h}\right),\\
&\text{HPT}: \ \Psi(z) = z\left[1 - \tfrac{1}{3}\left(\tfrac{z}{h/2}\right)^2\right].
\end{aligned}$$

In the first-order shear-deformation plate theory (FPT), the in-plane displacements are expanded up to the first term in the thickness coordinate, and the relations of normals to the mid-surface are assumed to be independent of the transverse deflection. For this theory we have

$$B_{ij} = B^a_{ij} = 0, \quad D^a_{ij} = F^a_{ij} = D_{ij}, \quad A^a_{ll} = hK_l\bar{c}_{ll}, \qquad (i, j = 1, 2, 6;\ l = 4, 5). \tag{22}$$

Note that the first condition in (2) is not satisfied; then the FPT yields a constant value of transverse shearing strain through the thickness of the plate, and thus requires shear-correction factors K_l in order to ensure the proper amount of transverse energy. The actual values of shear-correction coefficients of the present FPT are $K_4 = K_5 = 5/6$.

The HPT allows for a quadratic distribution of transverse shearing strain through the thickness of the plate by assuming a cubic expansion of the in-plane displacements in the thickness coordinate. The forms of the assumed displacement functions for both HPT and SPT are simplified by enforcing traction-free boundary conditions at the top and bottom surfaces of the plate. No shear-correction factors are needed for both theories, because a correct representation of the transverse shearing strain is given.

For the SPT, as well as for the HPT, the condition given in (2) must be satisfied. Also for the two theories, as in the FPT, we have $B_{ij} = B^a_{ij} = 0$. The FPT, SPT and HPT contain the same number of dependent variables. Those that are variationally consistent with both SPT and HPT involve additional higher-order stress resultants and material stiffness coefficients compared to the FPT.

The classical theory of thin plates (CPT) assumes that straight lines normal to the mid-surface before deformation remain straight and normal to the mid-surface after deformation, implying that transverse normal and shearing effects are negligible. For this theory, the buckling loads may be simply given as

$$S_0 = \frac{1}{S_{33}}\left[D_{11}\lambda^4 + 2\lambda^2\mu^2(D_{12} + 2D_{66}) + D_{22}\mu^4\right]P(t). \tag{23}$$

For the sake of completeness and comparison, the analytical solution for the stability problem of thin, isotropic, simply supported, rectangular elastic plates is presented here as given in most literature (see, *e.g.*, [24, pp. 351–360]):

$$S_1\frac{m^2\pi^2}{a^2}+S_2\frac{n^2\pi^2}{b^2}=D\left(\frac{m^2\pi^2}{a^2}+\frac{n^2\pi^2}{b^2}\right)^2, \tag{24}$$

where m and n are the mode numbers and

$$D=\frac{E_r h^3}{12(1-\nu_r^2)}, \tag{25}$$

is the flexural rigidity of the fully elastic plate with E_r and ν_r as Young's modulus and Poisson's ratio.

5. Generalized of Illyushin's approximation method

To solve the quasi-static problem of the linear theory for a viscoelastic composite material, we can use the method of reducing the non-homogeneous isotropic viscoelastic problem to a sequence of successive homogeneous anisotropic ones, as is done in the elastic case (see [13]).

For all theories considered, one can put (20) in the following form

$$S_0=F(m,n,\bar{\omega})P(t). \tag{26}$$

Thus, for each choice of m and n there is a corresponding unique value of S_0. The critical buckling load is the smallest of $S_0(m,n)$. For a given plate this value is dictated by a particular combination of the values of m and n, values of $\alpha, \zeta, \bar{\omega}$, and γ, plate geometry, and material properties.

In elastic composites F is a function of m, n and $\bar{\omega}$, while in viscoelastic composites it is an operator function of m, n and the time t. According to Illyushin's approximation method [13, 25, 26], the function F can be represented in the form

$$F(m,n,\bar{\omega})=\sum_{j=1}^{6} f_j(m,n)\,\Phi_j(\bar{\omega}), \tag{27}$$

where $\Phi_j\,(\bar{\omega})$ are some known kernels, constructed on the basis of the kernel $\bar{\omega}$ and may be chosen in the form

$$\Phi_1=1,\quad \Phi_2=\bar{\omega},\quad \Phi_3=\bar{\Pi}=\frac{1}{\bar{\omega}},\quad \Phi_4=\bar{g}_{\chi_1},\quad \Phi_5=\bar{g}_{\chi_2},\quad \Phi_6=\bar{g}_{\chi_3}. \tag{28}$$

The coefficients $f_j\,(m,n)$ are determined from the following system of algebraic equations

$$\sum_{j=1}^{6}\phi_{ij}\,f_j(m,n)=\Gamma_i(m,n),\qquad i=1,2,...,6, \tag{29}$$

where

$$\phi_{ij}=\int_0^1 \Phi_i(\bar{\omega})\,\Phi_j(\bar{\omega})\mathrm{d}\bar{\omega},\qquad \Gamma_i(m,n)=\int_0^1 \Phi_i(\bar{\omega})\,F(m,n,\bar{\omega})\mathrm{d}\bar{\omega}. \tag{30}$$

The viscoelastic solution may now be used to obtain explicit formulae for S_0 as functions of the mode numbers (m, n) and time t. Then,

$$\begin{aligned} S_0(m,n,\bar{\omega}) = {} & f_1 P(t) + f_2 \int_0^t \omega(t-\tau)\mathrm{d}P(\tau) + f_3 \int_0^t \Pi(t-\tau)\mathrm{d}P(\tau) \\ & + f_4 \int_0^t g_{\chi_1}(t-\tau)\mathrm{d}P(\tau) + f_5 \int_0^t g_{\chi_2}(t-\tau)\mathrm{d}P(\tau) + f_6 \int_0^t g_{\chi_3}(t-\tau)\mathrm{d}P(\tau). \end{aligned} \tag{31}$$

Taking $P(t) = P_0 H(t)$, where $H(t)$ is the Heaviside's unit step function,

$$H(t) = \begin{cases} 1 \ \ if \ \ t \geq 0, \\ 0 \ \ if \ \ t < 0, \end{cases} \tag{32}$$

we observe that the above formula takes the form

$$S_0(m,n,\bar{\omega}) = P_0[f_1 H(t) + f_2\omega(t) + f_3\Pi(t) + f_4 g_{\chi_1}(t) + f_5 g_{\chi_2}(t) + f_6 g_{\chi_3}(t)], \tag{33}$$

where $\omega(t) \equiv \bar{\omega}$, $\Pi(t) \equiv \bar{\Pi}$ and $g_{\chi_i}(t) \equiv \bar{g}_{\chi_i}$, $(i = 1, 2, 3)$ are given in Appendix A.

Assuming an exponential relaxation function

$$\omega(t) = c_1 + c_2\, e^{-t/t_s}, \tag{34}$$

where c_1 and c_2 are constants that are to be determined, and t_s is the relaxation time. With the help of the Laplace-Carson transform, the functions $\prod(t)$ and $g_{\chi_i}(t)$ are given in detail in Appendix B. They take the following forms:

$$\Pi(t) = \frac{1}{c_1}\left[1 - \frac{c_2}{c_1 + c_2}\,\mathrm{e}^{-c_1\tau/(c_1+c_2)}\right], \quad (\tau = t/t_s), \tag{35}$$

$$g_{\chi_i}(t) = \frac{1}{1 + c_1\chi_i}\left[1 - \frac{c_2\chi_i}{1 + (c_1 + c_2)\chi_i}\mathrm{e}^{-(1+c_1\chi_i)\tau/[1+(c_1+c_2)\chi_i]}\right]. \tag{36}$$

So, the final form of the buckling load in terms of the time parameter τ is

$$\begin{aligned} \beta_0(m,n,t) \ = \ & f_1 H(t) + f_2[c_1 + c_2 e^{-\tau}] + \frac{f_3}{c_1}\left[1 - \frac{c_2}{c_1 + c_2}\mathrm{e}^{-c_1\tau/(c_1+c_2)}\right] \\ & + f_4\,\bar{g}_{\chi_1} + f_5\,\bar{g}_{\chi_2} + f_6\,\bar{g}_{\chi_3}, \end{aligned} \tag{37}$$

where $\beta_0 = S_0/P_0$ and $\bar{g}_{\chi_i}$ are given in (36).

6. Comparison and results for viscoelastic composite plates

In this section, results obtained from the current HPT for several example problems are presented and compared with other theories. The results of the present investigations are given in Tables 2 and 3 and Figures 2–11. The value of Poisson's ratio of the reinforcement material was taken to be $\nu_r = 0{\cdot}3$. Note that we will assume in all of the analyzed cases (unless otherwise stated) that $\zeta = 10$, $\gamma = 0{\cdot}1$, $\bar{\omega} = 0{\cdot}5$, $c_1 = 0{\cdot}1$, $c_2 = 0{\cdot}9$, and $a/h = 10$. The appropriate value of the mode number n to get critical buckling is $n = 1$. With the help of the notation $\beta_0 = S_0/P_0$, the buckling parameter β $(\equiv \beta_0 a^2/D\pi^2)$, determined as per HPT is compared with those obtained by SPT, FPT and CPT. Note that the buckling parameter β is given in terms of the flexural rigidity of the fully-elastic plate D.

6.1. BUCKLING RESPONSE WITH CONSTANT KERNEL $\bar{\omega}$

When $\bar{\omega}$ takes a constant value, as mentioned in this section, $P(t)$ may be tends to a constant value P_0. In addition, all of the effective relaxation kernels $\bar{c}_{ij}$ are constants. Tables 2 and 3 are devoted to the buckling of viscoelastic composite plates and compare the present HPT results with those obtained as per SPT, FPT and CPT. Table 2 shows that the critical buckling loads of the present CPT for fully-elastic plates ($\gamma = 1$) are identical to those of Timoshenko and Gere [24, pp. 351–360] using the analytical solution for the stability problem of thin, isotropic, simply supported, rectangular elastic plates. In addition, the biaxial ($\alpha = 1$) and uniaxial ($\alpha = 0$) critical buckling loads using CPT are also exactly the same as those obtained by Lam *et al.* [27] without any foundation parameters.

Table 2. Non-dimensional critical buckling loads (β) of a reinforced viscoelastic square plate.

α	*a/h*	$\gamma = 1$ (4·0000)[a,b]			$\gamma = 0{\cdot}5$ (14·0365)[a]			$\gamma = 0$ (68·2500)[a]		
		FPT	SPT	HPT	FPT	SPT	HPT	FPT	SPT	HPT
0	2	1·6598	1·6811	1·6760	7·6008	7·6495	7·6364	30·5547	30·8818	30·8009
	4	2·9575	2·9626	2·9607	11·5510	11·5606	11·5564	52·1619	52·2351	52·2070
	5	3·2637	3·2666	3·2653	12·3330	12·3383	12·3356	56·9989	57·0395	57·0209
	10	3·7865	3·7869	3·7866	13·5660	135669	13·5662	65·0404	65·0470	65·0422
	20	3·9444	3·9445	3·9444	13·9157	13·9159	13·9157	67·4183	67·4196	67·4184
	50	3·9910	3·9910	3·9910	14·0170	14·0171	14·0170	68·1155	68·1157	68·1155

[a]Numbers in parenthesis based on CPT.
[b]Uniaxial critical buckling load is exactly the same as that obtained by Lam *et al.* [27].

Table 2. continued

α	*a/h*	$\gamma = 1$ (2·6667)[a,b]			$\gamma = 0{\cdot}5$ (9·3577)[a]			$\gamma = 0$ (45·5000)[a]		
		FPT	SPT	HPT	FPT	SPT	HPT	FPT	SPT	HPT
0·5	2	1·1065	1·1207	1·1173	5·0672	5·0997	5·0909	20·3698	20·5879	20·5339
	4	1·9717	1·9751	1·9738	7·7006	7·7070	7·7042	34·7746	34·8234	34·8046
	5	2·1758	2·1777	2·1769	8·2220	8·2256	8·2237	37·9992	38·0264	38·0139
	10	2·5243	2·5246	2·5244	9·0440	9·0446	9·0441	43·3603	43·3646	43·3615
	20	2·6296	2·6297	2·6296	9·2771	9·2773	9·2771	44·9455	44·9464	44·9456
	50	2·6607	2·6608	2·6607	9·3447	9·3447	9·3447	45·4104	45·4105	45·4104

[a]Numbers in parenthesis based on CPT.

Examination of the results depicted in Tables 2 and 3 reveals that, regardless of the considered values of the factors α and c, results obtained using HPT, SPT and FPT increase once a/h or/and a/b increase. The variation of results obtained as per HPT and FPT exhibits appreciable differences that increase when a/h decreases and a/b increases. In contrast to this behaviour, β determined in the framework of HPT and SPT show small differences between them, the differences becoming even smaller when β determined as per HPT (for thick and moderately thick rectangular plates) is compared to its SPT counterpart. So, SPT without using any shear correction factor gives results very close to HPT and closer than those obtained using FPT. In all cases, the results increase with the increase of the factors α and c and the maximum

Table 2. continued

α	*a/h*	$\gamma = 1$ (2·0000)[a,b]			$\gamma = 0{\cdot}5$ (7·0183)[a]			$\gamma = 0$ (34·1250)[a]		
		FPT	SPT	HPT	FPT	SPT	HPT	FPT	SPT	HPT
1	2	0·8299	0·8405	0·8380	3·8004	3·8248	3·8182	15·2773	15·4409	15·4005
	4	1·4788	1·4813	1·4804	5·7755	5·7803	5·7782	26·0810	26·1175	26·1035
	5	1·6319	1·6333	1·6327	6·1665	6·1692	6·1678	28·4994	28·5198	28·5105
	10	1·8932	1·8935	1·8933	6·7830	6·7834	6·7831	32·5202	32·5235	32·5211
	20	1·9722	1·9722	1·9722	6·9578	6·9579	6·9579	33·7091	33·7098	33·7092
	50	1·9955	1·9955	1·9955	7·0085	7·0085	7·0085	34·0578	34·0579	34·0578

[a]Numbers in parenthesis based on CPT.
[b]Biaxial critical buckling load is exactly the same as that obtained by Lam *et al.* [27].

Table 3. Non-dimensional critical buckling loads (β) of a reinforced viscoelastic rectangular plate under combined bending and compression ($a/h = 5$).

c	Theory	$a/b = 0{\cdot}5$			$a/b = 1{\cdot}0$			$a/b = 2{\cdot}0$		
		$\gamma = 1$	$\gamma = 0{\cdot}5$	$\gamma = 0$	$\gamma = 1$	$\gamma = 0{\cdot}5$	$\gamma = 0$	$\gamma = 1$[a]	$\gamma = 0.5$[b]	$\gamma = 0$[a]
1·5	CPT	6·2500	38·9894	308·1914	16·0000	56·1460	273·0000	64·0000	203·3413	1092·0000
	FPT	5·4777	35·3534	217·1190	13·0549	49·3321	227·9955	30·4545	145·3235	561·3474
	SPT	5·4801	35·3631	94·9631	13·0663	49·3533	228·1582	30·8665	145·8143	567·6887
	HPT	5·4788	35·3574	94·9445	13·0614	49·3424	228·0836	30·7683	145·6632	566·1340
1·0	CPT	3·1250	19·4947	53·3203	8·0000	28·0730	136·5000	32·0000	101·6707	546·0000
	FPT	2·7388	17·6767	47·4646	6·5275	24·6661	113·9977	15·2272	72·6617	280·6737
	SPT	2·7400	17·6816	47·4815	6·5332	24·6767	114·0791	15·4333	72·9071	283·8444
	HPT	2·7394	17·6787	47·4722	6·5307	24·6712	114·0418	15·3842	72·8316	283·0670
0·5	CPT	2·0833	12·9965	35·5469	5·3333	18·7153	91·0000	21·3333	67·7804	364·0000
	FPT	1·8259	11·7845	31·6431	4·3516	16·4440	75·9985	10·1515	48·4412	187·1158
	SPT	1·8267	11·7877	31·6544	4·3554	16·4511	76·0527	10·2888	48·6048	189·2296
	HPT	1·8263	11·7858	31·6482	4·3538	16·4475	76·0279	10·2561	48·5544	188·7113
0·0	CPT[c]	1·5625	9·7473	26·6602	4·0000	14·0365	68·2500	16·0000	50·8353	273·0000
	FPT	1·3694	8·8383	23·7323	3·2637	12·3330	56·9989	7·6136	36·3309	140·3368
	SPT	1·3700	8·8408	23·7408	3·2666	12·3383	57·0395	7·7166	36·4536	141·9222
	HPT	1·3697	8·8394	23·7361	3·2653	12·3356	57·0209	7·6921	36·4158	141·5335

[a]The mode in which the lowest (critical) buckling occurs is $m = 2$ for CPT and $m = 3$ for other shear deformation theories.
[b]The mode in which the lowest (critical) buckling occurs is $m = 2$ for shear deformation theories. Otherwise the critical buckling occurs in the first mode ($m = 1$).
[c]Results are exactly the same as those obtained by Timoshenko and Gere [24, pp. 351–360] using the analytical solution, $\gamma = 1$.

results occur at $\gamma = 0$ (for fully-viscoelastic plates). For a large value of the side-to-thickness ratio, *i.e.* $a/h = 50$, the difference between the values predicted by the shear deformation theories and CPT is not significant because the plate is essentially very thin. Once again, Table 3 shows that the uniaxial critical buckling loads ($\alpha = 0$) of the present CPT for fully-elastic plates ($\gamma = 1$) are identical to the exact values as calculated from the transcendental

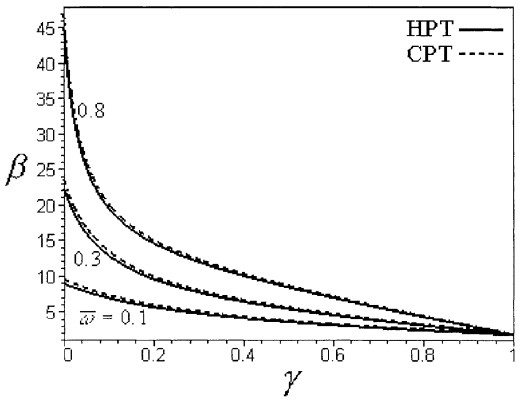

Figure 2. Effect of the volume fraction of fiber-reinforcement (γ) on the biaxial critical buckling (β) of a reinforced viscoelastic square plate for different values of the relaxation function $\bar{\omega}$ ($S_1 = S_2$).

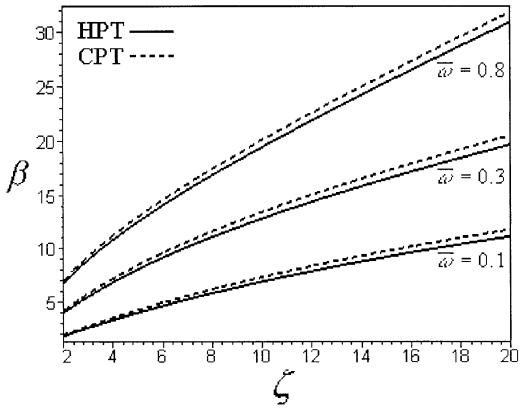

Figure 3. Effect of the constitutive parameter (ζ) on the biaxial critical buckling load (β) of a reinforced viscoelastic square plate for different values of the relaxation function $\bar{\omega}$ ($S_1 = S_2$).

equation of Timoshenko and Gere [24, pp. 351–360] using the analytical solution for the stability problem of thin, isotropic, simply supported, rectangular elastic plates.

Figures 2–8 are devoted to the buckling of viscoelastic composite plates using HPT. For comparison purposes, the results of CPT are also plotted. Figure 2 displays the variation of the biaxial buckling load β *vs.* the volume fraction of fiber- reinforcement γ for different values of the relaxation function $\bar{\omega}$. For all values of $\bar{\omega}$, the obtained results have the same values for fully-elastic plates ($\gamma = 1$). In addition, the maximum critical buckling occurs for fully-viscoelastic plates ($\gamma = 0$), and the results decrease as γ increases. The difference between the values predicted by HPT and CPT increases with the decrease of γ.

Figure 3 displays the variation of the biaxial buckling load β of the square plate *vs.* the constitutive parameter ζ for different values of $\bar{\omega}$. It is clear that the results increase with increase of ζ and $\bar{\omega}$. For all values of $\bar{\omega}$ the differences of biaxial buckling loads increase as ζ increases.

Figures 4 and 5 display, respectively, the variation of the uniaxial and biaxial buckling loads β of rectangular plates *vs.* the mode number *m*. For uniaxial buckling of square plates the critical value occurs, of course, at the first mode number ($m = 1$). This is not true for an aspect ratio larger than 1. For example, when $a/b = 2$ uniaxial critical buckling occurs at $m = 2$ (see also Table 3), while for $a/b = 3$ this critical value occurs at $m = 3$. However, the biaxial critical buckling load still occurs at the first mode number for all values of the aspect ratio. It should be noted that the errors between the results predicted by CPT and HPT increase with an increase of the mode number *m*.

Figure 6 shows the variation of the biaxial buckling load β *vs.* the aspect ratio a/b for different values of $\bar{\omega}$. The critical buckling increases with the increase of the aspect ratio and the relaxation function. For any value of $\bar{\omega}$ the difference between the critical buckling loads as predicted by HPT and CPT may be significant, especially for large values of a/b.

In Figure 7, the uniaxial and biaxial critical buckling loads of square plates are plotted against the side-to-thickness a/h ranging from 4 to 20. It should be noticed that the uniaxial critical buckling load may be twice the corresponding biaxial one. Also, the difference

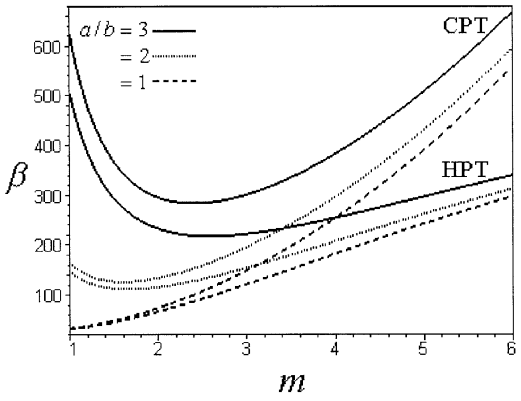

Figure 4. Effect of mode number (m) on the uniaxial buckling load (β) of a reinforced viscoelastic rectangular plate ($S_2 = 0$).

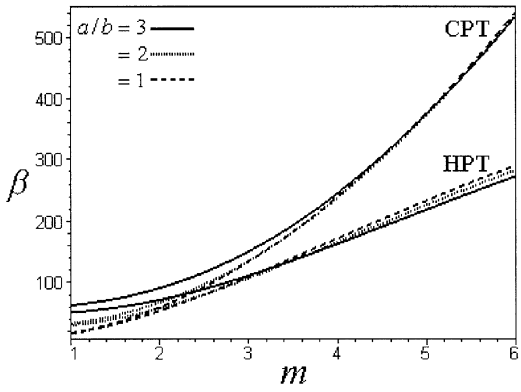

Figure 5. Effect of mode number (m) on the biaxial buckling load (β) of a reinforced viscoelastic rectangular plate ($S_1 = S_2$).

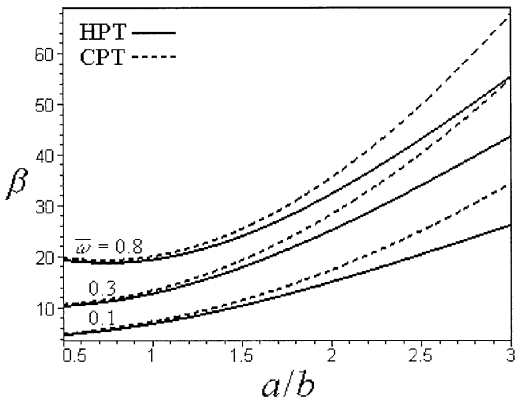

Figure 6. Effect of the aspect ratio (a/b) on the biaxial buckling load (β) of a reinforced viscoelastic rectangular plate ($S_1 = S_2$).

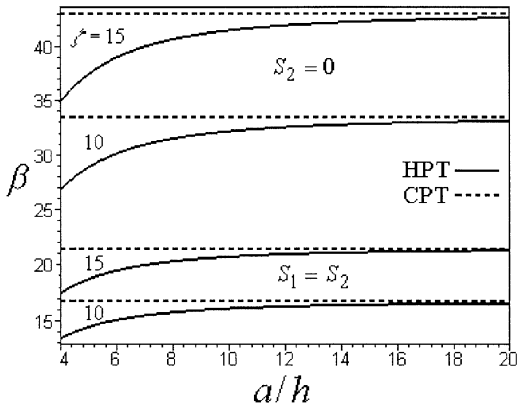

Figure 7. Effect of the side-to-thickness ratio (a/b) on the uniaxial ($S_2 = 0$) and biaxial ($S_1 = S_2$) critical buckling loads (β) of a reinforced viscoelastic square plate.

between the critical buckling loads predicted by HPT and CPT may be significant for all values of the side-to-thickness ratio. This difference increases, of course, when a/h decreases.

Finally, the buckling loads of reinforced viscoelastic rectangular plates under combined and compression *vs.* the aspect ratio are illustrated in Figure 8 for various values of the factor c. Obviously this figure reveals the sensitivity and symmetry of β to the variation of the factor c.

6.2. Time-dependence of buckling response

As particular examples for time-dependence, Figures 9–11 show the history of the biaxial critical buckling loads for various values of a/b, a/h, and γ, respectively. Some comments about the graphs are in order. Figure 9 reveals that the biaxial critical buckling load β of square plates decreases rapidly when $0 \leq \tau < 22$ for all values of a/h. For greater values of τ ($\tau \geq 25$), β may still be unchanged and this irrespective of the considered a/h ratio. In Figure 10 one can see the same behaviour of β as in Figure 8 in which β may still be constant

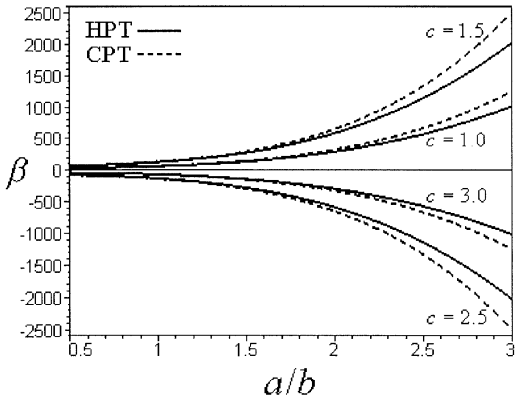

Figure 8. Effect of the aspect ratio (a/b) on the critical buckling load (β) of a reinforced viscoelastic rectangular plate under combined bending and compression ($m = 1$).

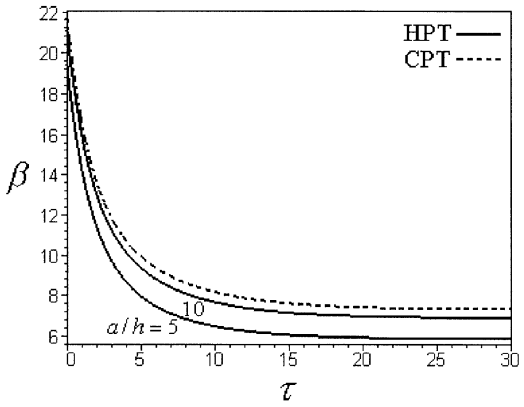

Figure 9. Effect of the time parameter (τ) on the biaxial critical buckling load (β) of a reinforced viscoelastic square plate for different values of the side-to-thickness ratio (a/h).

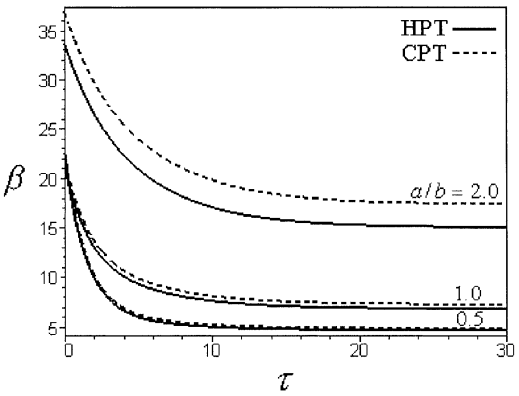

Figure 10. Effect of the time parameter (τ) on the biaxial critical buckling load (β) of a reinforced viscoelastic rectangular plate.

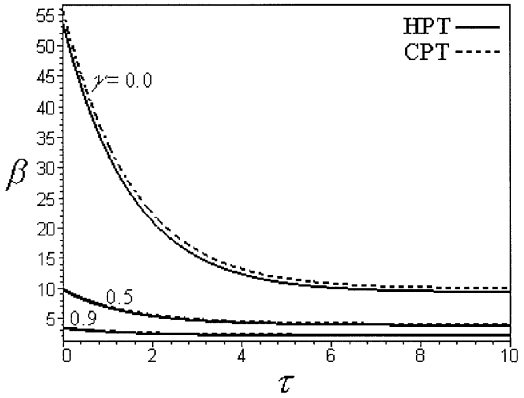

Figure 11. Effect of the time parameter (τ) on the biaxial critical buckling loads (β) of a reinforced viscoelastic square plate for different values of the volume fraction of fiber-reinforcement γ ($S_1 = S_2$).

for greater values of the volume fraction of $\tau_k(\tau \geq 25)$. Finally, the same behaviour of β *vs.* τ may be seen in Figure 11 for different values of γ. Results obtained using HPT and CPT for the purely viscoelastic case ($\gamma = 0$) may be independent of the time parameter when $\tau \geq 8$. For $\gamma = 0{\cdot}5$ results may still remain unchanged for $\tau \geq 5$. As expected, for large values of the fiber-reinforcement γ, the critical buckling loads are independent of the time parameter.

7. Conclusions

A generalized modal analysis approach is presented for the quasi-static stability analysis of fiber-reinforced viscoelastic composite plates. The governing equations of the classical, first-order, sinusoidal and higher-order theories are converted into a single-order system of equations. An exact eigenvalue buckling analysis of simply supported plates subjected to uni-

form and linearly varying uniaxial and uniform biaxial edge compression is obtained. Results compare well with those of the existing literature. As it is well known, the classical plate theory predicts critical buckling loads that are significantly different from those of the higher-order theory. The sinusoidal theory and the first-order theory results are very close to each other. However, the sinusoidal theory, as well as the higher-order theory, does not require the use of a shear-correction factor.

8. Appendix A

Young's moduli, Poisson's ratios and shear moduli used in (6) are presented here (see [13]). Consider a rectangular plate of parallel-packed parallelepipeds consisting of reinforcement and filler (see Figure 1). The ratio of the area occupied by reinforcement to the area of the entire plate at the cross-section $x = 0$ is denoted by γ (the volume fraction of fiber-reinforcement). The Young's moduli are given by

$$\bar{E}_x = \gamma E_r + (1-\gamma)E_f, \qquad \bar{E}_y = \frac{E_r E_f}{\gamma E_f + (1-\gamma)E_r}. \tag{A.1}$$

Taking into account the fact that $G_r = E_r/[2(1+\nu_r)]$ and $G_f = E_f/[2(1+\nu_f)]$, we have

$$\bar{G}_{xy} = \frac{G_r G_f}{\gamma G_f + (1-\gamma)G_r}, \tag{A.2}$$

for the shear modulus $\bar{G}_{xy}$. Similarly, the shear moduli $\bar{G}_{yz}$ and $\bar{G}_{xz}$ are given by

$$\bar{G}_{yz} = \bar{G}_{xy}, \qquad \bar{G}_{xz} = \gamma G_r + (1-\gamma)G_f. \tag{A.3}$$

Let us now determine the Poisson ratio $\bar{\nu}_{xy}$ in the case of a stretching of the plate along the *x*-axis; we obtain

$$\bar{\nu}_{xy} = \gamma\nu_r + (1-\gamma)\nu_f. \tag{A.4}$$

In the case of a stretching along the *y*-axis, we have

$$\bar{\nu}_{yx} = \frac{[\gamma\nu_r + (1-\gamma)\nu_f]E_r E_f}{[\gamma E_r + (1-\gamma)E_f][\gamma E_f + (1-\gamma)E_r]}. \tag{A.5}$$

Thus, it is obvious from (A.1), (A.4) and (A.5) that the reciprocal relation $\bar{\nu}_{xy}\bar{E}_y = \bar{\nu}_{yx}\bar{E}_x$ is fulfilled.

The filler material will be characterized by the bulk modulus K of the filler and kernel $\omega(t)$ if the filler possesses viscoelastic properties and the volume does not relax. Note that the viscoelastic modulus E_f and the corresponding Poisson ratio ν_f may be given in terms of the bulk (hydrostatic stress) modulus K and the kernel $\omega(t)$, which we will denote as $\bar{\omega}$, by

$$E_f = \frac{9K\bar{\omega}}{2+\bar{\omega}}, \qquad \nu_f = \frac{1-\bar{\omega}}{2+\bar{\omega}}. \tag{A.6}$$

Substitution of (A.6) in (A.1–A.5) gives

$$\bar{E}_x = E_r[\gamma + 9\zeta(1-\gamma)(1-\bar{g}_{\chi_1})], \tag{A.7}$$

$$\bar{E}_y = \frac{9E_r\zeta}{2(1-\gamma)\chi_2}(1-\bar{g}_{\chi_2}), \tag{A.8}$$

$$\bar{G}_{xy} = \bar{G}_{yz} = \frac{3E_r\zeta}{2(1-\gamma)\chi_3}(1-\bar{g}_{\chi_3}), \tag{A.9}$$

$$\bar{G}_{xz} = E_r\left[\frac{\gamma}{2(1+\nu_r)} + \frac{3}{2}(1-\gamma)\zeta\bar{\omega}\right], \tag{A.10}$$

$$\bar{\nu}_{xy} = \gamma\nu_r - (1-\gamma)\left(1-\frac{3}{2}\bar{g}_{\chi_1}\right), \tag{A.11}$$

and

$$\bar{\nu}_{yx} = \frac{9\zeta\bar{\nu}_{xy}}{[1-\gamma+9\zeta\gamma(1-\bar{g}_{\chi_1})][9\zeta(1-\gamma)+\gamma(1+\bar{\Pi})]}. \tag{A.12}$$

The notations

$$\zeta = \frac{K}{E_r}, \quad \bar{\Pi} = \frac{1}{\bar{\omega}}, \text{and } \bar{g}_{\chi_i} = \tfrac{1}{1+\chi_i\bar{\omega}}, \quad (i=1,2,3), \tag{A.13}$$

are introduced here, in which

$$\chi_1 = \frac{1}{2}, \qquad \chi_2 = \frac{1}{2}\left(1+\frac{9\gamma\zeta}{1-\gamma}\right), \qquad \chi_3 = \frac{3\gamma\zeta(1+\nu_r)}{1-\gamma}. \tag{A.14}$$

9. Appendix B

The Laplace-Carson transform can be used to determine the functions $\Pi(t)$ and $g_{\chi_i}(t)$ as given in (37) and (38). Denoting the transforms of $\Pi(t)$ and $g_{\chi_i}(t)$ by $\Pi^*(s)$ and $g^*_{\chi_i}(s)$, respectively, we may deduce the Laplace-Carson transform of $\omega(t)$ as follows:

$$\omega^*(s) = s\int_0^\infty \omega(t)\mathrm{e}^{-st}\mathrm{d}t. \tag{B.1}$$

Using (34), one obtains

$$\omega^*(s) = s\int_0^\infty \left(c_1\mathrm{e}^{-st} + c_2\mathrm{e}^{-(s+1/t_s)t}\right)\mathrm{d}t, \tag{B.2}$$

or

$$\omega^*(s) = c_1 + c_2\frac{s}{s+1/s_t}. \tag{B.3}$$

But we have

$$\Pi^*(s) = \frac{1}{\omega^*(s)} = \frac{1}{c_1 + c_2 s/(s+1/t_s)}, \tag{B.4}$$

or

$$\Pi^*(s) = \frac{1}{c_1}\left(1-c_3\frac{s}{s+c_4}\right), \tag{B.5}$$

where

$$c_3 = \frac{c_2}{c_1 + c_2}, \qquad c_4 = \frac{c_1}{(c_1 + c_2)t_s}. \tag{B.6}$$

Then we can find the function $\Pi(t)$ by using the inverse Laplace-Carson transform of (B.5) in the form

$$\Pi(t) = \frac{1}{c_1}\left(1 - c_3 e^{-c_4 t}\right) = \frac{1}{c_1}\left[1 - \frac{c_2}{c_1 + c_2} e^{-c_1 \tau/(c_1+c_2)}\right], \quad (\tau = t/t_s). \tag{B.7}$$

Similarly

$$g^*_{\chi_i}(s) = \frac{1}{1 + \chi_i \omega^*(s)} = \frac{1}{1 + \chi_i\left[c_1 + c_2\left(\frac{s}{s+1/s_i}\right)\right]}, \tag{B.8}$$

or

$$g^*_{\chi_i}(s) = \frac{1}{1 + c_1\chi_i}\left(1 - c_5 \frac{s}{s + c_6}\right), \tag{B.9}$$

where

$$c_5 = \frac{c_2\chi_i}{1 + (c_1 + c_2)\chi_i}, \quad c_6 = \frac{1 + c_1\chi_i}{[1 + (c_1 + c_2)\chi_i]t_s}. \tag{B.10}$$

Also the function $g_{\chi_i}(t)$ can be found by using the inverse Laplace-Carson transform of (B.9). Then, one obtains

$$g_{\chi_i}(t) = \frac{1}{1 + c_1\chi_i}\left(1 - c_5 \mathrm{e}^{-c_6 t}\right), \tag{B.11}$$

or in final form:

$$g_{\chi_i}(t) = \frac{1}{1 + c_1\chi_i}\left[1 - \frac{c_2\chi_i}{1 + (c_1 + c_2)\chi_i} \mathrm{e}^{-(1+c_1\chi_i)\tau/[1+(c_1+c_2)\chi_i]}\right]. \tag{B.12}$$

References

1. Z. Hashin, The elastic moduli of heterogeneous materials. *J. Appl. Mech. Trans. ASME* 84E (1962) 143–150.
2. Z. Hashin and S. Shtrikman, A variational approach to the theory of the elastic behavior of multiphase materials. *J. Mech. Phys. Solids* 11 (1963) 127–140.
3. Z. Hashin, On elastic behavior of fiber reinforced materials of arbitrary transverse phase geometry. *J. Mech. Phys. Solids* 13 (1965) 119–134.
4. Z. Hashin, Viscoelastic behavior of heterogeneous media. *J. Appl. Mech. Trans. ASME* 32E (1965) 630–636.
5. S. Ahmed and F. R. Jones, A review of particulate reinforcement theories for polymer composites. *J. Mater. Sci.* 25 (1990) 4933–4942.
6. D. W. Wilson and J. R. Vinson, Viscoelastic analysis of laminated plate buckling. *AIAA J.* 22 (1984) 982–988.
7. C. G. Kim and C. S. Hong, Viscoelastic sandwich plates with cross-ply faces. *J. Struct. Engng.* 114 (1988) 150–164.
8. N. N. Huang, Viscoelastic buckling and postbuckling of circular cylindrical laminated shells in hygrothermal environment. *J. Marine Sci. Tech.* 2 (1994) 9–16.
9. H. H. Pan, Vibrations of viscoelastic plates. *J. de Mécanique* 5 (1966) 355–374.
10. L. Librescu and N. K. Chandiramani, Dynamic stability of transversely isotropic viscoelastic plates. *J. Sound Vibr.* 130 (1989) 467–486.

11. A. M. Zenkour, Analytical solution for bending of cross-ply laminated plates under thermo-mechanical loading. *Comp. Struct.* 65 (2004) 367–379.
12. K. P. Soldatos and T. Timarci, A unified formulation of laminated composite, shear deformable, five-degrees-of-freedom cylindrical shell theories. *Comp. Struct.* 25 (1993) 165–171.
13. B. E. Pobedrya, Structural anisotropy in viscoelasticity. *Polymer Mech.* 12 (1976) 557–561.
14. E. Reissner and Y. Stavsky, Bending and stretching of certain types of heterogeneous aelotropic elastic plates. *J. Appl. Mech.* 28 (1961) 402–408.
15. J. M. Whitney, *Structural Analysis of Laminated Anisotropic Plates*. Lancaster, PA: Technomic, (1987) 356 pp.
16. A. M. Zenkour, Exact mixed-classical solutions for the bending analysis of shear deformable rectangular plates. *Appl. Math. Modelling* 27 (2003) 515–534.
17. K. H. Lo, R. M. Christensen and E. M. Wu, A high-order theory of plate deformation: Part 1, homogeneous plates; Part 2, laminated plates. *J. Appl. Mech.* 44 (1977) 663–676.
18. M. Levinson, An accurate, simple theory of the statics and dynamics of elastic plates. *Mech. Res. Comm.* 7 (1980) 343–350.
19. J. N. Reddy, A simple higher-order theory of laminated composite plates. *J. Appl. Mech.* 51 (1984) 745–752.
20. J. N. Reddy, *Theory and Analysis of Elastic Plates*. Philadelphia: Taylor & Francis (1999) 576 pp.
21. M. E. Fares and A. M. Zenkour, Buckling and free vibration of non-homogeneous composite cross-ply laminated plates with various plate theories. *Compos. Struct.* 44 (1999) 279–287.
22. A. M. Zenkour, Natural vibration analysis of symmetrical cross-ply laminated plates using a mixed variational formulation. *Eur. J. Mech. A/Solids* 19 (2000) 469–485.
23. A. M. Zenkour, Buckling and free vibration of elastic plates using simple and mixed shear deformation theories. *Acta Mech.* 146 (2001) 183–197.
24. S. P. Timoshenko and J. M. Gere, *Theory of Elastic Stability*. New York: McGraw-Hill (1961) 541 pp.
25. M. N. M. Allam and A. M. Zenkour, Bending response of a fiber-reinforced viscoelastic arched bridge model. *Appl. Math. Modelling* 27 (2003) 233–248.
26. M. N. M. Allam and A. M. Zenkour, Stress concentration factor of structurally anisotropic composite plates weakened by an oval opening. *Compos. Struct.* 61 (2003) 199–211.
27. K. Y. Lam, C. M. Wang and X. Q. He, Canonical exact solutions for Levy-plates on two-parameter foundation using Green's functions. *Engng. Struct.* 22 (2000) 364–378.